A simple and efficient FDTD/PBC algorithm for scattering analysis of periodic structures

Fan Yang,[1] Ji Chen,[2] Rui Qiang,[2] and Atef Elsherbeni[1]

Received 19 May 2006; revised 22 February 2007; accepted 8 May 2007; published 11 July 2007.

[1] An efficient finite difference time domain (FDTD) algorithm with a simple periodic boundary condition (PBC) is developed to analyze reflection and transmission properties of general periodic structures with arbitrary incident angles. In this new approach, the FDTD simulation is performed by setting a constant horizontal wave number instead of a specific incident angle. The principle of the FDTD/PBC algorithm is discussed and two important implementation issues are addressed, namely, the excitation of plane wave and the suppression of horizontal resonance. The validity of the approach is demonstrated through several numerical examples on dielectric slabs and frequency selective surfaces.

Citation: Yang, F., J. Chen, R. Qiang, and A. Elsherbeni (2007), A simple and efficient FDTD/PBC algorithm for scattering analysis of periodic structures, *Radio Sci.*, *42*, RS4004, doi:10.1029/2006RS003526.

1. Introduction

[2] Periodic electromagnetic structures have received increased attentions in recent years for their applications in the design of frequency selective surfaces (FSS), electromagnetic band gap (EBG) structures, and negative index materials. The finite-difference time-domain (FDTD) method has been used to analyze these structures. To take advantage of the periodic replication of these structures, periodic boundary conditions (PBC) was developed and implemented in various forms so that only a single unit needs to be simulated [*Maloney and Kesler*, 2000]. Some representative PBCs include the Sin-Cosine method [*Harms et al.*, 1994], the unit cell shifting method [*Holter and Steyskal*, 1999], the split-field method [*Roden et al.*, 1998], and the spectral FDTD method [*Aminian and Rahmat-Samii*, 2004].

[3] In this paper, a simple and efficient FDTD/PBC algorithm is presented to analyze the reflection and transmission properties of periodic structures. Compared to many previous PBC techniques, a distinguish feature of the proposed algorithm is that periodic structures are simulated under a constant horizontal wavenumber instead of at a given incident angle. The idea of FDTD computation with constant wavenumbers was originated in the analysis of guided wave structures and eigenvalue problems [*Xiao et al.*, 1992; *Cangellaris et al.*, 1993], and then expanded to the plane wave scattering problems in [*Aminian and Rahmat-Samii*, 2004]. The novelty of this paper is the direct computation of E and H fields rather than the indirect calculation using auxiliary fields [*Aminian et al.*, 2005]. Thus, the conventional Yee's scheme is used to update the E and H fields. As a consequence, the proposed method possesses several advantages, such as the simplicity in the algorithm implementation, the same stability condition and numerical errors as those of the conventional FDTD method, and good computational efficiency near the grazing incident angles.

[4] The implementation procedure of the proposed FDTD/PBC algorithm is discussed and two key issues are addressed. The first one is the plane wave excitation in this algorithm. Since the new algorithm uses a constant horizontal wavenumber instead of an incident angle, the conventional plane wave incident approach is no longer applicable. Alternatively, a one-field plane wave excitation approach is proposed in this paper. For example, only horizontal E incident field is incorporated for the TE^z plane wave case and only horizontal H incident field for the TM^z case. The second implementation issue is the horizontal resonance associated with the numerical scheme. Due to the implementation of periodic boundary conditions (PBC), the energy exits from one side PBC will re-enter the computational domain from the opposite side PBC. Thus, if a wave propagates horizontally, its energy will not be absorbed by the perfectly matched layers (PML). As a consequence, a horizontal resonance occurs and the fields never decay to zero in the time domain. It is revealed

[1]Department of Electrical Engineering, University of Mississippi, University, Mississippi, USA.
[2]Department of Electrical and Computer Engineering, University of Houston, Houston, Texas, USA.

0048-6604/07/2006RS003526

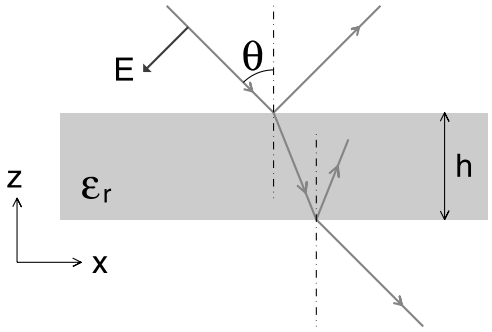

Figure 1. A plane wave impinges upon a dielectric slab. The incident angle of the TM^z wave is denoted by θ. The dielectric slab has a thickness (h) of 9.375 mm and dielectric constant (ε_r) of 2.56.

in this paper that the horizontal resonance can be suppressed by properly designing the excitation waveforms.

[5] The developed algorithm is used to analyze several periodic structures such as a dielectric slab and a frequency selective surface (FSS) consisting of dipole elements. The simulation results are compared with analytical results, results from a split field FDTD method, and results from commercial software such as Ansoft HFSS and Designer. Good agreement between these results is observed, which demonstrates the validity and accuracy of the new algorithm.

2. FDTD/PBC Algorithm

[6] The novel FDTD/PBC algorithm is developed based on the comprehension of the k_x-frequency plane. In this section, we first discuss the reflection coefficient in the k_x-frequency plane, and then explain the rationale of the constant k_x method. The implementation of the FDTD/PBC algorithm is described afterward.

2.1. Reflection Coefficient in the k_x-Frequency Plane

[7] A dielectric slab is first analyzed as an example to illustrate the reflection coefficient in the k_x-frequency plane. Figure 1 shows a TM^z plane wave illuminating a dielectric slab of thickness h and dielectric constant ε_r. Assuming the incident angle is θ, the horizontal wave number k_x is determined as below:

$$k_x = k_0 \cdot \sin\theta, \tag{1}$$

where $k_0 = 2\pi f\sqrt{\varepsilon_0\mu_0}$ is the free space wave number. The reflection coefficient of the dielectric slab is calculated analytically and plotted in the k_x-frequency plane, as shown in Figure 2. The horizontal axis represents the wave number along the x direction (k_x), and vertical axis represents the frequency. The magnitude of the reflection coefficient (Γ) is represented by different dark scales as indicated by the scale bar on the right. The k_x-frequency plane is separated into the evanescent wave region ($k_x^2 > k_0^2$) and plane wave region ($k_x^2 < k_0^2$) by the light line ($k_x = k_0$). For our applications, only the reflection coefficient in the plane wave region needs to be considered. The normal incidence and an oblique incidence cases are also denoted by the dashed lines in Figure 2.

[8] It is observed that the total transmission, represented by dark scales, occurs in two regions. The first region starts at 10 GHz when k_x equals to zero (normal incidence). The frequency increases to 12 GHz as the horizontal wave number increases. The second region is around a tilted line in the k_x-frequency plane, which corresponds to an incident angle of 58°, the Brewster angle for this case. It is clear that the reflection coefficient plot in the k_x-frequency plane provides a complete and clear vision on the scattering property of the dielectric slab for all incident angles.

2.2. Rationale of the Constant k_x Method

[9] Using this k_x-frequency plane, we introduce the rationale of the constant k_x method and compare it with various PBCs. For a periodic structure with periodicity of a along the x direction, the periodic boundary condition of the electric and magnetic fields in the frequency domain is expressed as below:

$$\begin{aligned} \mathrm{E}(x=0,y,z) &= \mathrm{E}(x=a,y,z)\exp(jk_xa) \\ \mathrm{H}(x=0,y,z) &= \mathrm{H}(x=a,y,z)\exp(jk_xa) \end{aligned}. \tag{2}$$

Here, k_x is the horizontal wave number determined by both the frequency and incident angle through (1). When (2) is directly transformed into the time domain,

$$\begin{aligned} E(x=0,y,z,t) &= E(x=a,y,z,t+a\sin\theta/C) \\ H(x=0,y,z,t) &= H(x=a,y,z,t+a\sin\theta/C) \end{aligned}, \tag{3}$$

where C is the free space wave speed. It is noticed that the field data in the future time step are needed to update electric and magnetic fields in the current time step, which creates a fundamental challenge in formulating periodic boundary conditions (PBC).

[10] For a normal incident case, we have $\theta = 0$ and $k_x = 0$. Since there is no need for time advancement in this situation, the periodic boundary condition for normal incidence can be implemented in FDTD method without any difficulties. To simulate oblique incidences the Sin-Cosine method was developed in [*Harms et al.*, 1994], but only a single frequency is calculated per simulation as indicated by a plus sign in Figure 2. To improve the computation efficiency and obtain a wideband response per simulation, the split field method [*Roden et al.*, 1998] was developed based on field transformation technique

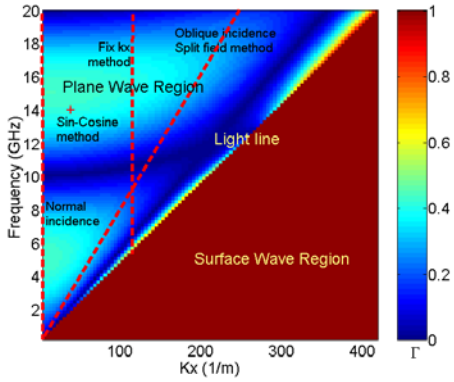

Figure 2. Reflection coefficient of the dielectric slab in the k_x-frequency plane, which is calculated analytically. Various methods to model periodic boundary conditions in FDTD simulations are also indicated in the k_x-frequency plane by the dashed lines and the plus sign.

[*Veysoglu et al.*, 1993]. This method is capable to calculate oblique incidence on a tilted line in Figure 2, but the time step size used in such FDTD simulations needs to be decreased as the incident angle increases. In addition, the split field method needs relatively complex formulations for the updating scheme and absorbing boundary conditions.

[11] An alternative approach to formulate the PBC is to choose a constant horizontal wave number instead of a specified incident angle in the FDTD simulations. The relationship of the horizontal wave number, frequency, and incident angle is described in (1). When a constant k_x is chosen, change of frequency leads to corresponding change of the incident angle. The advantage of choosing a constant k_x is recognized from the transformation of (2) into the time domain, where a very simple periodic boundary condition (PBC) can be obtained:

$$\begin{aligned} E(x=0,y,z,t) &= E(x=a,y,z,t)\exp(jk_xa) \\ H(x=0,y,z,t) &= H(x=a,y,z,t)\exp(jk_xa) \end{aligned} \quad . \tag{4}$$

Note that $\exp(jk_xa)$ is a constant number in (4). Therefore, no time delay or advancement is required in this equation. Compared to traditional methods, this technique calculates the reflection coefficient along a vertical dashed line in the k_x-frequency plane, as show in Figure 2. It also should be pointed out that both E and H fields have complex values in the FDTD computation because of the PBC in (4).

[12] The physical meaning of this technique can be understood using the principle of superposition. For a given k_x, time domain equation (4) is true for each frequency component. Thus, when a wideband pulse is launched into a linear system, (4) still holds by the superposition of all frequency components.

2.3. Plane Wave Excitation

[13] The implementation of the FDTD/PBC algorithm is simple and straightforward. The electric and magnetic fields are computed as follows:

[14] 1. In the interior of computational domain, the conventional Yee's scheme is used to update the electromagnetic fields [*Taflove and Hagness*, 2000].

[15] 2. At the periodic boundaries of the computational domain, (4) is used to update the EM fields. Perfectly matched layers (PML) are used to truncate the computational domain along the z direction, as shown in Figure 3. Note that periodic boundary condition (4) is also applied in the PML regions.

[16] One important issue related to the proposed algorithm is the excitation of plane waves in the computational domain. The traditional approach is to use the total-field/scattered field technique [*Taflove and Hagness*, 2000], where both incident electric and magnetic fields need to be incorporated on the interface between the total field and scattered field regions. When this technique is applied in the constant k_x method, a difficulty occurs regarding the incident angle. For example, if a TM^z wave

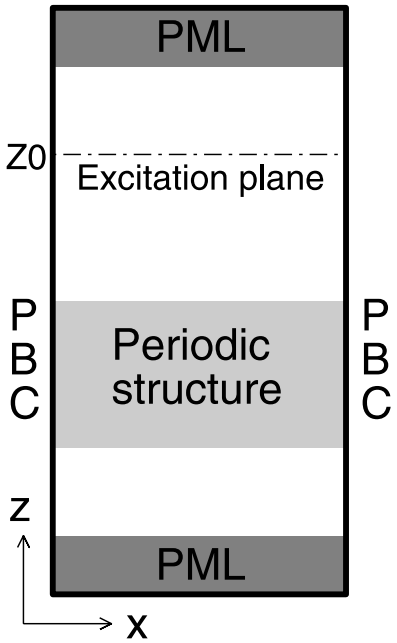

Figure 3. FDTD computational domain of a periodic structure, which is truncated by perfectly matched layers (PML) along the z direction and periodic boundary conditions (PBC) in the horizontal directions. The plane wave incidence is added on the excitation plane at $z = z_0$.

illuminates upon a periodic structure, the tangential incident fields H_y^{inc} and E_x^{inc} are expressed below:

$$\begin{aligned} H_y^{inc} &= H_0 \\ E_x^{inc} &= -\eta H_0 \cos\theta = -\eta H_0 \sqrt{1-(k_x/k_0)^2}, \end{aligned} \tag{5}$$

where η is the wave impedance in free space. It is noticed that E_x component depends on the incident angle. Since in the proposed algorithm, k_x is fixed and the incident angle θ varies with frequency, it is not easy to transform the E_x in (5) into the time domain. To solve this difficulty, the traditional Total-Field/Scattered-Field (TF/SF) technique is modified: only the H_y component is added on the excitation plane for the TM^z case. As a consequence of the one-field excitation technique, the plane wave is excited to propagate not only into $z < z_0$ region but also into $z > z_0$ region. Thus, the entire computational domain becomes the total field region and there is no scattered field region. The scattered field can be calculated by the difference of total field and incident field. Similar strategy applies for TE^z case: only the E_y component is added on the excitation plane. For general polarizations, it is required to break it up into TE and TM components, but both components can be excited and computed simultaneously.

[17] On the excitation plane, the incident field adopts a modulated Gaussian waveform and the phase delay along the x direction should be inserted:

$$H_y^{inc}(x,t) = \exp\left[-\frac{(t-t_0)^2}{2\sigma_t^2}\right] \exp(j2\pi f_0 t) \exp(-jk_x x). \tag{6}$$

The parameters of the modulated Gaussian waveform are the time delay t_0, center frequency f_0, and pulse width σ_t. The time delay t_0 is set to a value between $3\sigma_t$ to $5\sigma_t$ for a smooth transition in time domain excitation. For convenience, a frequency bandwidth BW is defined below:

$$\mathrm{BW} \times 2\pi \equiv 2 \cdot \left(3\sigma_f\right) = 2 \cdot \frac{3}{\sigma_t}. \tag{7}$$

From the definition above, the signal magnitude at $f_0 \pm$ (BW/2) is 40 dB lower than the signal level at the center frequency f_0.

2.4. Horizontal Resonance

[18] The developed excitation technique is first used to stimulate the propagation of a plane wave in free space in order to demonstrate its validity. The center frequency is set to 10 GHz and the bandwidth is set to 20 GHz. Two horizontal observation planes are set 12.5 mm apart to study the propagation behavior. Figures 4a–4c show the real parts of electric fields at two observation planes for k_x = 0, 100.6, and 174.2 radian/m, respectively. When k_x = 0, the plane wave is normally incident into the computation domain and a constant time delay is observed between two observation plane. When k_x = 100.6 radian/m, the plane wave is obliquely incident into the computational domain and the incident angle varies with frequency. A time delay is also observed, but more importantly an oscillation appears at the late time. Similar phenomenon is observed in Figure 4c, where k_x = 174.2 radian/m. The E field levels at both observational planes do not decay to zero even though the excitation signal vanishes at a late time. As a consequence, the calculation of the reflection and transmission coefficients in the frequency domain will be deteriorated by these oscillations.

[19] To understand this problem, the behavior of the oscillation is analyzed and it is found that the oscillation frequencies in Figures 4b and 4c are 4.8 GHz and 8.3 GHz, respectively. At these frequencies, $k_0 = k_x$ and $\theta = 90°$. Thus, the plane wave propagates horizontally. A feature of the horizontal wave is that the E fields on two observation planes should be in phase with each other, which is noticed in Figures 4b and 4c. The energy of the horizontal wave continuously re-enters the computational domain through the periodic boundary condition instead of being absorbed by the top and bottom PML. As a consequence, the fields do not decay to zero and an oscillation is observed. The magnitude of the oscillation is determined by the strength of the excitation signal at the resonant frequency. Since 8.3 GHz is closer to the center frequency 10 GHz and a stronger signal is excited, the oscillation magnitude in Figure 4c is larger than that in Figure 4b.

[20] To suppress the horizontal resonance, various approaches can be implemented such as designing a frequency notch waveform. In this paper, a simple method is used by shifting the center frequency of the modulated Gaussian waveform. Figure 4d presents the FDTD simulated E fields with f_0 = 16 GHz, BW = 20 GHz, and k_x = 100.6 radian/m. The resonant frequency (4.8 GHz) is now outside the Gaussian bandwidth. Therefore, the horizontal resonance is small enough to be neglected and an accurate transmission coefficient can be obtained in the frequency domain. In practice, the center frequency can be chosen using following equation:

$$f_0 = f_r + \frac{\mathrm{BW}}{2} = \frac{k_x C}{2\pi} + \frac{\mathrm{BW}}{2}, \tag{8}$$

where f_r is the resonant frequency of the horizontal wave. In free space, the f_r is calculated from the horizontal wave number k_x and free space wave speed C. Equation (8) also indicates that the signal strength is concentrated in the

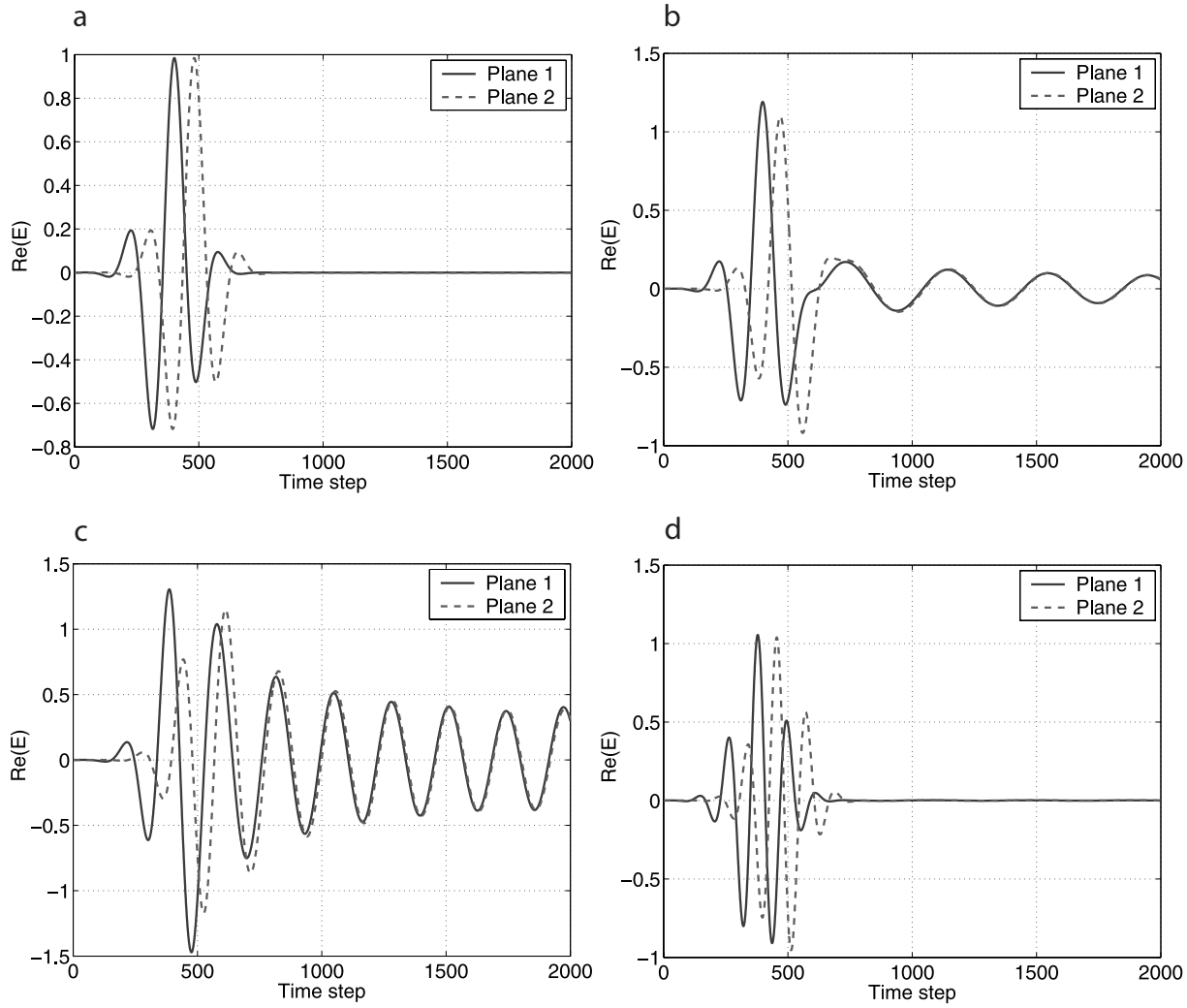

Figure 4. FDTD simulation of plane wave propagation in free space. (a) f_0 = 10 GHz, BW = 20 GHz, k_x = 0; (b) f_0 = 10 GHz, BW = 20 GHz, k_x = 100.6; (c) f_0 = 10 GHz, BW = 20 GHz, k_x = 174.2; (d) f_0 = 16 GHz, BW = 20 GHz, k_x = 100.6. The horizontal resonance can be suppressed by choosing a proper center frequency and signal bandwidth.

frequency range above the light line, which is in the plane wave region as shown in Figure 2.

3. Numerical Examples and Discussions

3.1. Example 1: A Dielectric Slab

[21] The developed algorithm is first used to analyze the dielectric slab shown in Figure 1 because an infinite dielectric slab can be considered as a periodic structure with arbitrary periodicity. To obtain a good resolution in the k_x-frequency plane, reflection coefficients are calculated at 100 distinct k_x values ranging from 0 to 419 (radian/m). The FDTD simulation is repeated for 100 times and each simulation outputs the reflection coefficient on a vertical line in the k_x-frequency plane. The obtained reflection coefficient as a function of both k_x and frequency is plotted in Figure 5a, where the half wavelength transmission and the Brewster angle transmission can be clearly visualized. Figure 5b compares the analytical and FDTD computed reflection coefficients at several k_x values. The good agreement demonstrates the validity of the new algorithm.

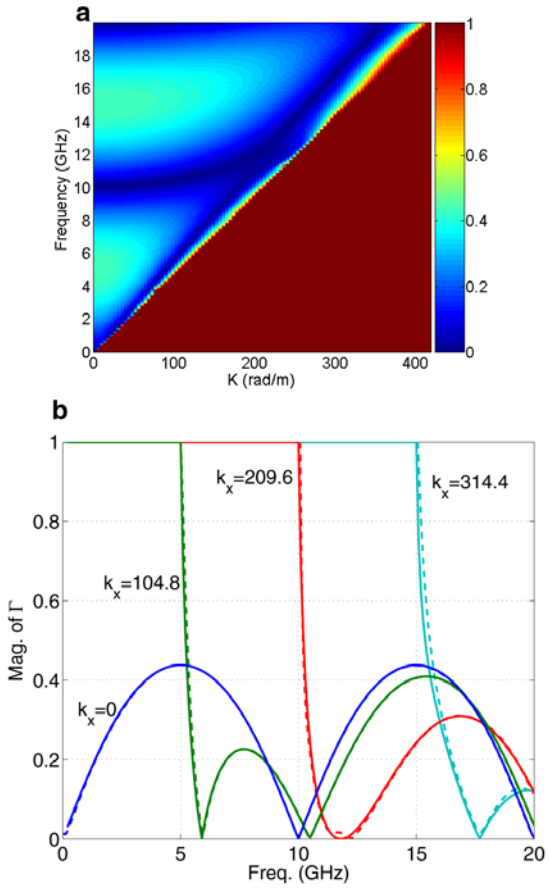

Figure 5. (a) Reflection coefficient of the dielectric slab computed using the proposed FDTD/PBC algorithm. (b) Comparisons between the FDTD/PBC results (dashed line) with analytical results (solid lines) for different k_x values.

3.2. Example 2: A Dipole Frequency Selective Surface (FSS)

[22] The constant k_x method is then applied to characterize the reflection coefficient of a frequency selective surface (FSS) that consists of dipole elements [*Munk*, 2000]. The thin periodic dipole array resides on a dielectric slab with a thickness h and dielectric constant ε_r, as shown in Figure 6. The parameters of the periodic structure are provided in the caption, which are the same as those given in [*Gianvittorio et al.*, 2003]. A TE^z plane wave impinges on the periodic structure in the x-z plane. The FDTD simulation is performed 100 times using different values of k_x sampled along the axis of horizontal wave number. The calculated reflection coefficients are plotted in Figure 7. Strong reflection is represented by the white color and transmission region is denoted by the dark zone. The first reflected region occurs around 9 GHz and the frequency of total reflection slightly decreases as k_x increases, which

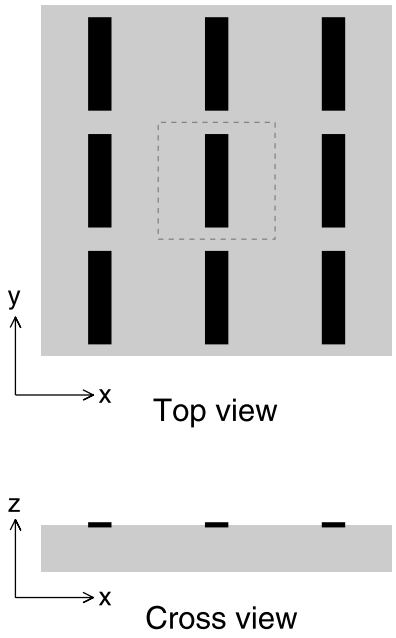

Figure 6. Geometry of a frequency selective surface (FSS) consisting of dipole elements. The dipole length is 12 mm and width is 3 mm. The periodicity is 15 mm in both the x and y directions. The substrate has a thickness of 6 mm and dielectric constant of 2.2.

agrees with the observation in [*Pelton and Munk*, 1979]. The first transmission region starts at 16 GHz for normal incidence ($k_x = 0$). When k_x increases, both the transmission frequency and the magnitude of the transmission coefficient decrease. It is also observed from Figure 7 that the second reflection region immediately follows the first transmission region. Transmission and reflection at multiple Floquet modes occur at frequencies higher than 16 GHz.

[23] One can also extract curves of the reflection coefficient versus frequency at any given incident angles

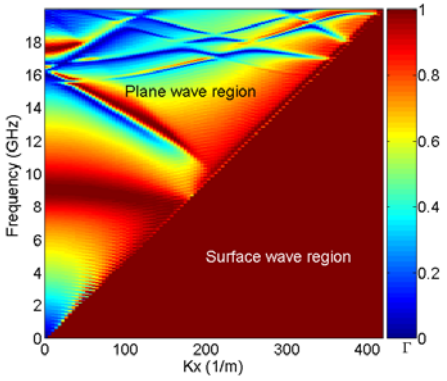

Figure 7. The reflection coefficient of the dipole FSS computed using the proposed FDTD/PBC algorithm.

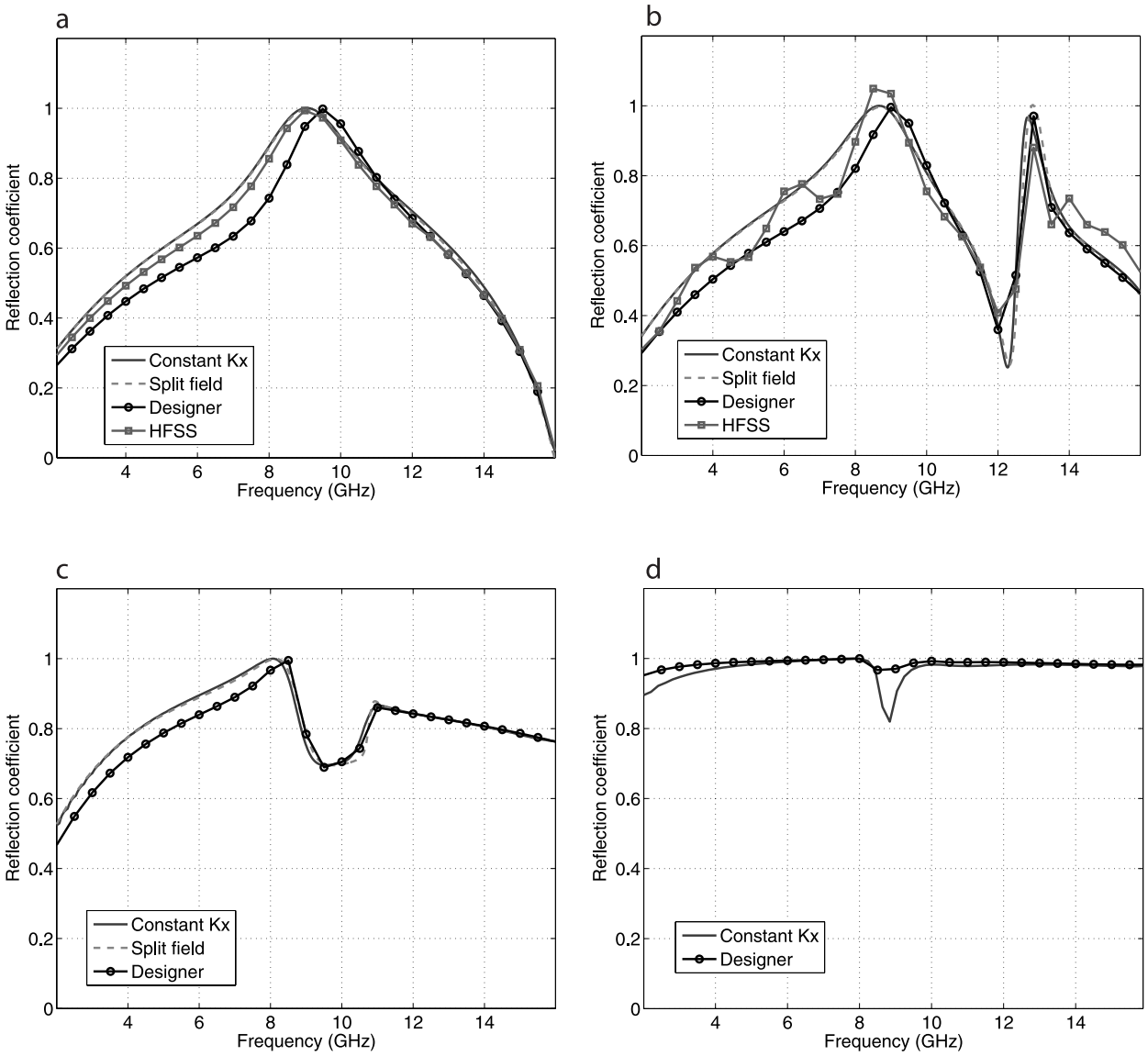

Figure 8. Reflection coefficients of the dipole FSS at several incident angles: (a) 0°, (b) 30°, (c) 60°, and (d) 85°.

from the data on k_x-frequency plane using an interpolation scheme. For a give incident angle θ and frequency f, the horizontal wavenumber k_x can be calculated from (1). Assuming that k_{x1} and k_{x2} ($k_{x1} < k_x < k_{x2}$) are sampled horizontal wavenumbers closest to k_x, the reflection coefficient Γ at k_x is calculated as follows:

$$\Gamma(f, k_x) = \frac{\Gamma(f, k_{x1}) \cdot (k_{x2} - k_x) + \Gamma(f, k_{x2}) \cdot (k_x - k_{x1})}{k_{x2} - k_{x1}} \tag{9}$$

For example, the reflection coefficients for the incident angles of 0°, 30°, 60°, and 85° are extracted and plotted in Figure 8.

[24] To verify the accuracy of the new algorithm, the same structure is analyzed using three different programs. One is the split field program developed by H. Mosallaei at University of California, Los Angeles [*Mosallaei and Rahmat-Samii*, 2003]. The other two are Ansoft HFSS program and Ansoft Designer program. The split field program is based on the FDTD method, the HFSS program is based on the Finite Element

Method (FEM), and the Designer program is based on the Method of Moment (MoM). All three programs compute the reflection coefficient at given incident angles. Good agreements between different methods are observed, especially at small incident angles. As the incident angle increases, the HFSS results become unstable. When the incident angle is close to 90°, the split field FDTD method cannot give a converged result.

[25] It is also interesting to compare the memory usage and computational time of different methods. The memory used by our proposed algorithm, HFSS program, and Designer program are 4 Mb, 230 Mb, and 81 Mb, respectively, whereas the memory usage for the split field method is not reported by the program. In term of the computational time, our program spends 75 seconds for each k_x line on a computer with an Intel Xeron 3.00 GHz CPU, and total calculation time for the complete k_x-frequency plane (100 k_x) is around 2 hours. Using the same computer, the HFSS and Designer spend around 750 and 670 seconds for each incident angle (including 29 frequency points). The computational time of the split field method varies with the incident angle. As the angle increases from 0° to 30° and 60°, the time increases from 778 seconds to 950 seconds and 2589 seconds. It should be pointed out that the above comparisons can only be used as a reference because the programs are developed by different agents.

3.3. Advantages of the Proposed FDTD/PBC Algorithm

[26] The validity of the new FDTD/PBC algorithm has been demonstrated in the preceding examples. It is worthwhile to emphasize several important advantages of this new approach. First, the new algorithm is very easy to implement. In contrast to the field transformation methods that use auxiliary fields [*Roden et al.*, 1998; *Aminian et al.*, 2005], the new approach computes E and H fields directly. Thus, no complicated discretization formulas need to be derived and the traditional Yee's updating scheme is used to calculate field values, as outlined in section 2.3. In addition, the perfectly matched layers remain unchanged, which also helps to simplify the implementation procedure.

[27] Another advantage of the new algorithm is the efficiency in calculating the scattering at large incident angles. When the field transformation methods such as the split field technique are used to calculate the oblique incidence, the time step size (Δt) needs to be decreased as the incident angle (θ) increases. To satisfy the stability constrains, the time step size and incident angle for square cells and free space should follow the inequality below [*Maloney and Kesler*, 2000],

$$\frac{C\Delta t}{\Delta x} \le \frac{1-\sin\theta}{\sqrt{3}}. \tag{10}$$

Δx is the size of the FDTD grid cell. The time step size approaches zero when the incident angle goes to 90°. For example, when Δx is 1 mm in the FSS analysis, $\Delta t < 1.925 \times 10^{-12}$ (second) is required for normal incidence. For a large incident angle such as 85°, $\Delta t < 7.323 \times 10^{-15}$ (second) is necessary. Therefore, the simulation time becomes prohibitively long for the latter one.

[28] In contrast, the constant k_x method presented in this paper uses a standard Yee's scheme to update the E and H fields. The stability condition remains unchanged regardless of the horizontal wave number (k_x) or incident angle, as expressed below [*Taflove and Hagness*, 2000]:

$$\frac{C\Delta t}{\Delta x} \le \frac{1}{\sqrt{3}}. \tag{11}$$

For the FSS example, a constant $\Delta t = 1.667 \times 10^{-12} < 1.925 \times 10^{-12}$ (second) is used for all k_x values. Therefore, the new approach has a good computational efficiency, especially for plane wave scattering at large incident angles. This analysis also explains the computation time differences between the constant k_x method and the split field method discussed in section 3.2.

4. Conclusion

[29] This paper presents a novel technique to model the periodic boundary condition (PBC) in the FDTD method. By choosing a constant k_x value in FDTD simulations, a wide band response of the reflection coefficient can be obtained. The reflection coefficient in the k_x-frequency plane is computed through several rounds of FDTD simulations using different k_x values. The new approach is easy to implement and efficient in analyzing plane wave scattering from arbitrary incident angles. The validity of the approach has been demonstrated through the good agreements between the FDTD simulation results and the data obtained from analytical method and various numerical programs.

[30] **Acknowledgments.** The author would like to thank the reviewers for the constructive comments that helped to improve the quality of the paper.

References

Aminian, A., and Y. Rahmat-Samii (2004), Spectral FDTD: a novel computational technique for the analysis of periodic structures, *Proc. IEEE Antennas Propag. Soc. Symp.*, *3*, 3139–3142.

Aminian, A., F. Yang, and Y. Rahmat-Samii (2005), Bandwidth determination for soft and hard ground planes by spectral FDTD: a unified approach in visible and surface wave regions, *IEEE Trans. Antennas Propag.*, *53*(1), 18–28.

Cangellaris, A. C., M. Gribbons, and G. Sohos (1993), A hybrid spectral/FDTD method for electromagnetic analysis of guided

waves in periodic structures, *IEEE Microwave Guided Wave Lett.*, *3*(10), 375–377.

Gianvittorio, J., J. Romeu, S. Blanch, and Y. Rahmat-Samii (2003), Self-similar prefractal frequency selective surfaces for multiband and dual-polarized applications, *IEEE Trans. Antennas Propag.*, *51*(11), 3088–3096.

Harms, P., R. Mittra, and W. Ko (1994), Implementation of the periodic boundary condition in the finite-difference time-domain algorithm for FSS structures, *IEEE Trans. Antennas Propag.*, *42*, 1317–1324.

Holter, H., and H. Steyskal (1999), Infinite phased-array analysis using FDTD periodic boundary conditions-pulse scanning in oblique directions, *IEEE Trans. Antennas Propag.*, *47*, 1508–1514.

Maloney, J., and M. P. Kesler (2000), Analysis of periodic structures, *Computational Electrodynamics: The Finite Difference Time Domain Method*, 2nd ed., edited by A. Taflove and S. Hagness, Artech House, Boston.

Mosallaei, H., and Y. Rahmat-Samii (2003), Periodic bandgap and effective dielectric materials in electromagnetics: characterization and applications in nanocavities and waveguides, *IEEE Trans. Antennas Propag.*, *51*(3), 549–563.

Munk, B. A. (2000), *Frequency Selective Surface*, John Wiley, New York.

Pelton, E. L., and B. A. Munk (1979), Scattering from periodic arrays of crossed dipoles, *IEEE Trans. Antennas Propag.*, *27*(3), 323–330.

Roden, J. A., S. D. Gedney, M. P. Kesler, J. G. Maloney, and P. H. Harms (1998), Time-domain analysis of periodic structures at oblique incidence: orthogonal and nonorthogonal FDTD implementations, *IEEE Trans. Microwave Theory Tech.*, *46*(4), 420–427.

Taflove, A., and S. Hagness (2000), Incident wave source conditions, *Computational Electrodynamics: The Finite Difference Time Domain Method*, 2nd ed., Artech House, Boston.

Veysoglu, M. E., R. T. Shin, and J. A. Kong (1993), A finite-difference time-domain analysis of wave scattering from periodic surfaces: oblique incidence case, *J. Electromagn. Waves Appl.*, *7*, 1595–1607.

Xiao, S., R. Vahldieck, and H. Jin (1992), Full-wave analysis of guided wave structures using a novel 2-D FDTD, *IEEE Microwave Guided Wave Lett.*, *2*(5), 165–167.

A. A.Elsherbeni and F. F.Yang, Department of Electrical Engineering, University of Mississippi, University, MS 38677, USA. (atef@olemiss.edu; fyang@olemiss.edu)

J. J.Chen and R. R.Qiang, Department of Electrical and Computer Engineering, University of Houston, Houston, TX 77204, USA. (jchen18@uh.edu; rui.qiang@mail.uh.edu)